Hindawi
Geofluids
Volume 2023, Article ID 9945428, 9 pages
https://doi.org/10.1155/2023/9945428

Research Article

A Prediction Model Based on the Long Electrode Source for Fault Anomaly in Tunnel

Daiming Hu,[1,2] **Hao Liu**,[1,2] **Xiaodong Yang**,[3] **and Mingxin Yue**[4]

[1]*PowerChina Zhongnan Engineering Corporation Limited, Changsha 410019, China*
[2]*Hunan Province Key Laboratory of Hydropower Development Key Technology, Changsha 410019, China*
[3]*School of Earth and Space Sciences, University of Science and Technology of China, Hefei 230026, China*
[4]*College of Transportation Engineering, Nanjing Tech University, Nanjing 210009, China*

Correspondence should be addressed to Hao Liu; 330633026@qq.com and Mingxin Yue; staryue@126.com

Received 21 February 2023; Revised 28 March 2023; Accepted 12 May 2023; Published 20 May 2023

Academic Editor: Yu Wang

The resistivity method has been widely used to predict the water-bearing structure of tunnels. The traditional resistivity uses the point electrode (PE) source in the tunnel to excite the electric field. Because the tunnel face is inaccessible, its exploration depth is limited and small. In order to overcome this problem, the horizontal pilot hole is used as the long electrode (LE) source in the tunnel. We use the finite element method (FEM) to establish a three-dimensional modeling algorithm for tunnel detection using a long electrode source. The accuracy of the algorithm is verified by using the long electrode source model. By a lot of numerical simulations, a prediction model of a long electrode source for tunnel detection is firstly proposed. The predicted results show that it has good applicability in detecting long-distance anomaly. The comparison of the long electrode source and point electrode source models shows that the detection depth of the long electrode prediction model is farther than that of the point electrode source. This long electrode source method can improve the construction efficiency and effectively prevent water inrush in the tunnel.

1. Introduction

The resistivity method of PE source in tunnel is becoming more and more popular, which has been applied in environmental investigation, coal mining, and subway tunnel engineering [1–3]. In some mountainous areas with deep tunnels, there often occurs water inrush in front of the tunnel face. Predicting the location of water inrush is a very tough task for construction enterprises before tunnel excavation. To ensure construction safety, the prediction of the complex geological structure must be accurate, because the rich-water fault structure ahead of the tunnel face is very dangerous, which could bring huge difficulties to the tunnel excavation [4].

At present, the resistivity method of PE source in tunnel has become more and more popular. Because the resistivity method has the features of low-cost and portable equipment, and it is very sensitive to water-rich faults, the resistivity method has been an indispensable way for predicting water inrush structures, such as karst caves [5].

However, there is a shortcoming for the PE resistivity method existing a small detection depth for the water-rich disaster anomaly in the geological hazard survey of the tunnel. It is because that the electric signal induced by the PE source is easy to be disturbed from ambient noise in detecting large-distance structure, but it has a good detecting effect in superficial structure. But for deep structure, the way of PE source is easily disturbed by tunnel conditions [6, 7]. Another one reason is the inaccessible tunnel face, which limited the PE source to be close to the anomaly. During tunnel excavation, surveyors often use horizontal pilot boreholes for observation. Therefore, we can use the horizontal pilot drilling as a LE source, which can inject a strong current near the fault anomaly. The LE source may be developed as a new method to detect the water inrush structure to increase detection depth.

Although the LE source has been widely used in the typical geological model by the resistivity method prospecting for more than 30 years [8–10], the resistivity method of the LE source is only used in ideal half-space models and one-dimensional layered models. So far, introducing a LE source into the whole-space model of the tunnel for predicting water inrush fault structure has not been published in the previous literature. Some people suggest that in practical work, the point source resistivity method is suitable for detecting short-distance disaster anomalies, and it is better to use a long electrode source resistivity method for long-distance anomalies [11, 12].

The goal of this study is to propose a new prediction model with the LE source resistivity method based on finite element mesh for detecting water inrush fault in the tunnel, which can guide engineer before practical tunnel excavation to locate the potential water-rich fault in front of the tunnel. The finite element method has become an important tool widely used for the modeling of the resistivity method in the past decades [13–30]. Here, we use the finite element method to implement the 3D modeling of the LE source in the tunnel.

The structure of this study is divided into the following parts. First, we describe the boundary condition and the basic equation of the tunnel model with LE source and apparent resistivity formulas. Next, the LE model proves the accuracy of the algorithm, and then we discuss the numerical simulation of several models under different parameters with the LE source and the comparison with the PE source model. In the end, the conclusion is made.

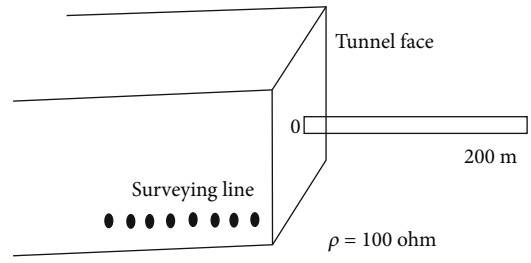

Figure 1: A LE source model.

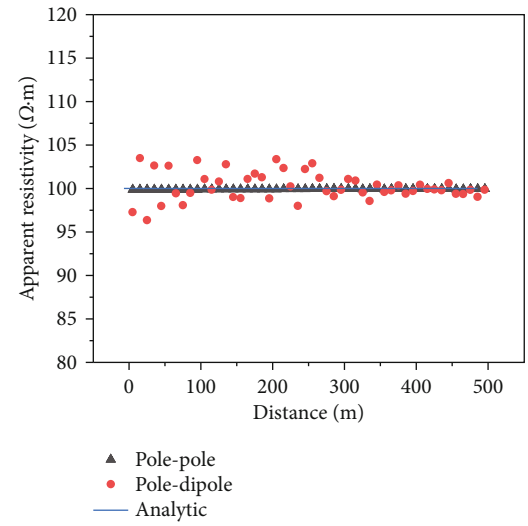

Figure 2: Analytic and numerical results on two configurations.

2. Numerical Module

2.1. The Basic Equations. The boundary condition between the air and the tunnel satisfies the Neumann boundary condition on the surface domain, and it satisfies the third boundary condition on the infinite domain. The basic equation and boundary conditions of the point source can be seen [31, 32]. The LE source is assumed as a collection of point elements. The modeling of the total electrical field excited by a point source has been solved [27]. The function of the LE source variational problem could be converted by assembling those PE sources [33].

$$F_L[u] = \int_L \left\{ \int_\Omega \left[\frac{1}{2}\sigma(\nabla u)^2 - u\nabla j\left(\vec{r}\right) \right] d\Omega + \frac{1}{2}\int_{\partial\Omega} \sigma \frac{\cos\left(\vec{r},\vec{n}\right)}{\vec{r}} u^2 dS \right\} \mathrm{dl}. \tag{1}$$

$F_L[u]$ is a function of the scalar potential u, σ is the conductivity, j is the current density, $\vec{r}$ is the observed position, $\vec{n}$ is the normal vector, L is the LE source, Ω is the model space. Equation (1) using a linear function can be written.

$$F_L[u] = \sum_{e=1}^{N_e} \left(\frac{1}{2} U_e^T K_e^1 U_e + \frac{1}{2} U_e^T K_e^2 U_e - U_e^T p \right). \tag{2}$$

Here,

$$p = \int_L \int_{\Omega_e} \nabla j\left(\vec{r}\right) \mathrm{Ndvdl}. \tag{3}$$

U_e is the element potential, N_e is the element number, K_e^1 is the volume element matrix, N is the shape function, K_e^2 is the face element matrix, p represents the LE source components, Ω_e indicates each tetrahedral element. All local system equations were assembled into a global system equation to form a large system linear equation [34, 35]. The computational problem of this large system equation could be solved by a conjugate gradient method [19].

2.2. Apparent Resistivity of LE Source. For tunnel prediction, the computational formulas under the pole-pole configuration of the LE source have been given [36].

$$\begin{aligned} u_N &= \frac{G_N}{4\pi L} \bullet \mathrm{I}\rho, \\ \rho_s &= \frac{4\pi L}{G_N} \bullet \frac{u_N}{I}. \end{aligned} \tag{4}$$

u_N is the potential, G_N is the configuration coefficient, and ρ_s is apparent resistivity.

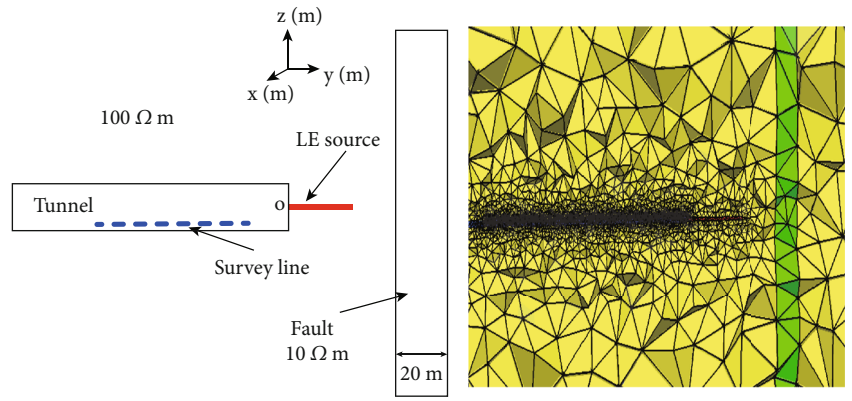

Figure 3: Schematic diagram of fault anomaly in the tunnel on the LE source and the FE grid used in the modeling.

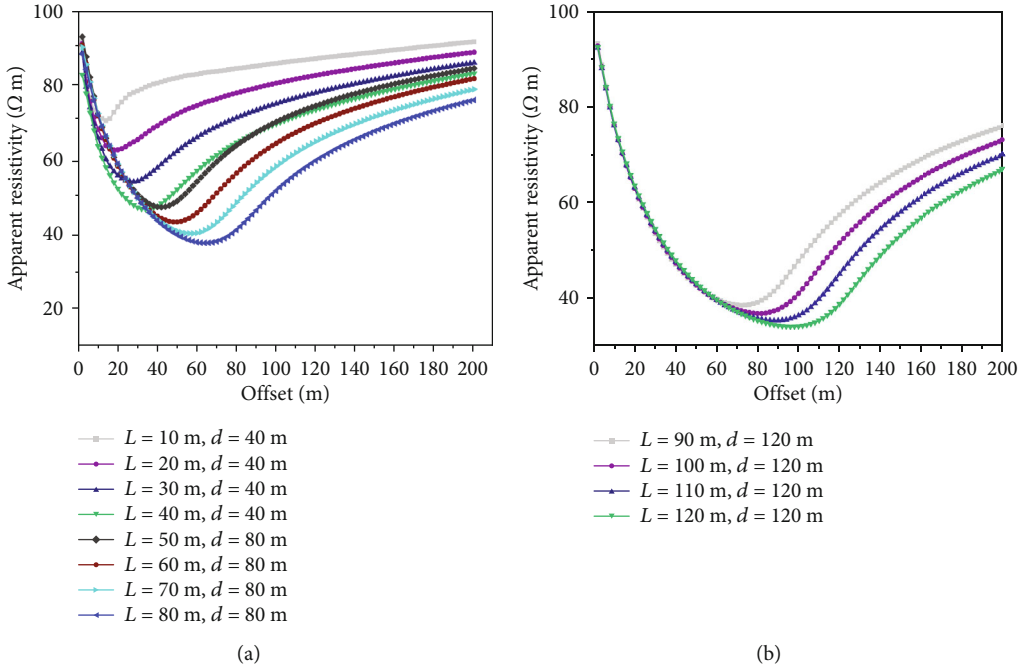

Figure 4: Apparent resistivity of different LE sources.

For pole-dipole configuration, the computational formulas of the LE source at M and N could be transformed

$$\Delta u_{\mathrm{MN}} = \left(\frac{G_M}{4\pi L} - \frac{G_N}{4\pi L}\right) I\rho,$$
$$\rho_s^* = \left(\frac{G_M}{4\pi L} - \frac{G_N}{4\pi L}\right)^{-1} \frac{\Delta u_{\mathrm{MN}}}{I}. \tag{5}$$

More detailed procedures also can be seen in reference [36].

3. Verification of the Algorithm

The following case was calculated on a PC with 11th Gen Intel(R) Core(TM) i7-11700 @ 2.50 GHz and 16 GB RAM.

To check the accuracy of the LE source algorithm, a LE source was simulated in a uniform surrounding rock with the resistivity of 100 Ω m in Figure 1. There are 50 observed electrodes with the interval of 10 m on the surveying line. The location of the LE source is placed at point O. We use two pole-pole and pole-dipole configurations to test the feasibility of the LE algorithm. The whole model with 621769 tetrahedra and 87742 nodes is used by unstructured mesh [37, 38].

We test the accuracy of the LE source model under two pole-pole and pole-dipole configurations in the surveying line of the tunnel floor. As Figure 2 shown, in the surveying line, numerical apparent resistivity calculated by the LE model under two configurations is consistent with the analytical value of 100 Ω m. Besides, the precision of the pole-pole configuration is better than that of the pole-dipole configuration. They prove the feasibility of our LE algorithm.

4. Numerical Simulations

We simulated several fault models using the LE source, which is closely related to practical tunneling work. The goal of the study is to propose a prediction model using LE source configuration in locating fault ahead of the tunnel.

4.1. Prediction Model of the LE Source. To study the prediction performance of the LE source device used in detecting fault anomaly in the tunnel, a fault model is designed in Figure 3, and the model parameters are as follows. The tunnel face area is 4 m × 4 m, the air of the tunnel has a resistivity of $10^8\,\Omega$ m, and a lot of potential electrodes are placed at the tunnel floor with the interval of 2 m. The LE source is located at point O. The surrounding rock is 100 Ω m and fault is 10 Ω m. The thickness of the fault is 20 m, and the depth of the tunnel is 500 m. The whole model domain is enough large. By adjusting the real horizontal distance between the tunnel face and the left boundary of the fault (d = 40 m, 80 m, 120 m) and the length of the LE source (L = 10 m, 20 m, 30 m, ⋯, 110 m, 120 m), we calculated multigroup fault models with different lengths of LE sources and different horizontal distances.

Figure 4 shows apparent resistivity curves for different LE sources and different horizontal fault distances of 40 m, 80 m, and 120 m, respectively. Under the condition of the same fault distance, as the LE source becomes longer, the minimum value of the curves becomes lower, and the offset ($x_{\min}$) of the minimum apparent resistivity also becomes larger. Because the longer the LE source is, the closer it is to the actual fault anomaly, which can excite a stronger electric signal and is easily coupled with the high-conductivity anomaly. In the traditional data processing, there is a linear relationship between the observed offset $x_{\min}$ and the actual horizontal distance d, which was used to estimate the position of the anomaly in the tunnel. It is particularly emphasized here, for the modeling at L = 40 m and d = 40 m, d = 40.1 m is actually simulated in the algorithm to keep the LE source as close as possible with fault anomaly. The same approximation was processed in the following similar cases. It is because that when the LE source crosses the two layers (nonuniform conductive medium), the current density distribution of the LE surface will change with the difference of the conductivities of both media. So far, there is no analytic solution of current density in a nonuniform conductive medium. However, there is an approximate current density distribution formula that some researchers proposed [33]. The numerical algorithm in this section is not applicable to the LE source passing through an inhomogeneous medium if it contacts the boundary of fault anomaly. That is, when the LE source passes through two different inhomogeneous media, the propagation equation of current density needs to be deduced again. It is worth noting that if there is an underlaid anomaly beneath the tunnel floor, it will generate a minimum and maximum fluctuation on apparent resistivity curves and interfere with the prediction of anomaly positions ahead of the tunnel face.

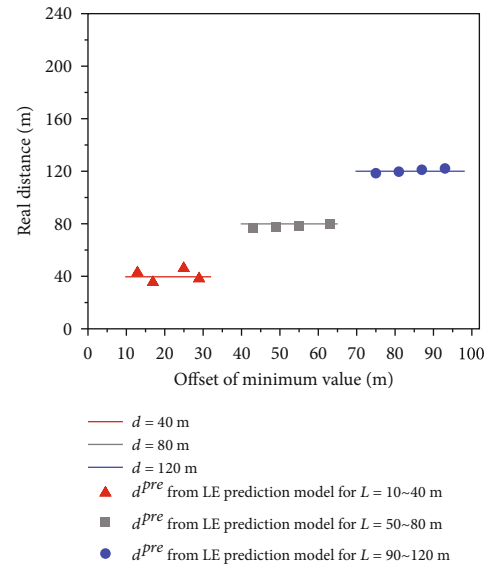

Figure 5: Results of LE prediction model.

Table 1: The influence of real distance and length of LE source on apparent resistivity curve and their prediction distances and errors.

Distance (m)	Offset (m)	Length (m)	Predicted distance (m)	Error (%)
d = 40	$x_{\min}$ = 13	L = 10	d^{pre} = 43.75	-3.75
d = 40	$x_{\min}$ = 17	L = 20	d^{pre} = 35.83	4.16
d = 40	$x_{\min}$ = 25	L = 30	d^{pre} = 46.33	-6.33
d = 40	$x_{\min}$ = 29	L = 40	d^{pre} = 38.40	1.59
d = 80	$x_{\min}$ = 43	L = 50	d^{pre} = 76.53	3.46
d = 80	$x_{\min}$ = 49	L = 60	d^{pre} = 77.82	2.17
d = 80	$x_{\min}$ = 55	L = 70	d^{pre} = 79.10	0.89
d = 80	$x_{\min}$ = 63	L = 80	d^{pre} = 80.39	-0.39
d = 120	$x_{\min}$ = 75	L = 90	d^{pre} = 118.52	1.47
d = 120	$x_{\min}$ = 81	L = 100	d^{pre} = 119.80	0.19
d = 120	$x_{\min}$ = 87	L = 110	d^{pre} = 121.09	-1.09
d = 120	$x_{\min}$ = 93	L = 120	d^{pre} = 122.38	-2.38

Figure 4 shows the calculated offset results ($x_{\min}$) for water-rich faults at different real horizontal distances (d = 40 m, 80 m, 12 m) and different lengths of the LE source (L = 10 m, 20 m, 30 m, ⋯, 110 m, 120 m). On these numerical results, we proposed an equation by a multivariable linear regression method as follows:

$$d^{\text{pre}} = f(x_{\min}, L) = \text{a}x_{\min} + bL + \text{c}. \tag{6}$$

d^{pre} denotes the predicted distance of the water-rich fault anomaly ahead of the tunnel, $x_{\min}$ is the offset corresponding to abscissa of the minimum apparent resistivity value, three coefficients are a = 4.605, b = −2.634, and c = 10.235, respectively. Statistics results show that the fitting R-square is equal to 0.992, indicating that this equation is highly feasible. This

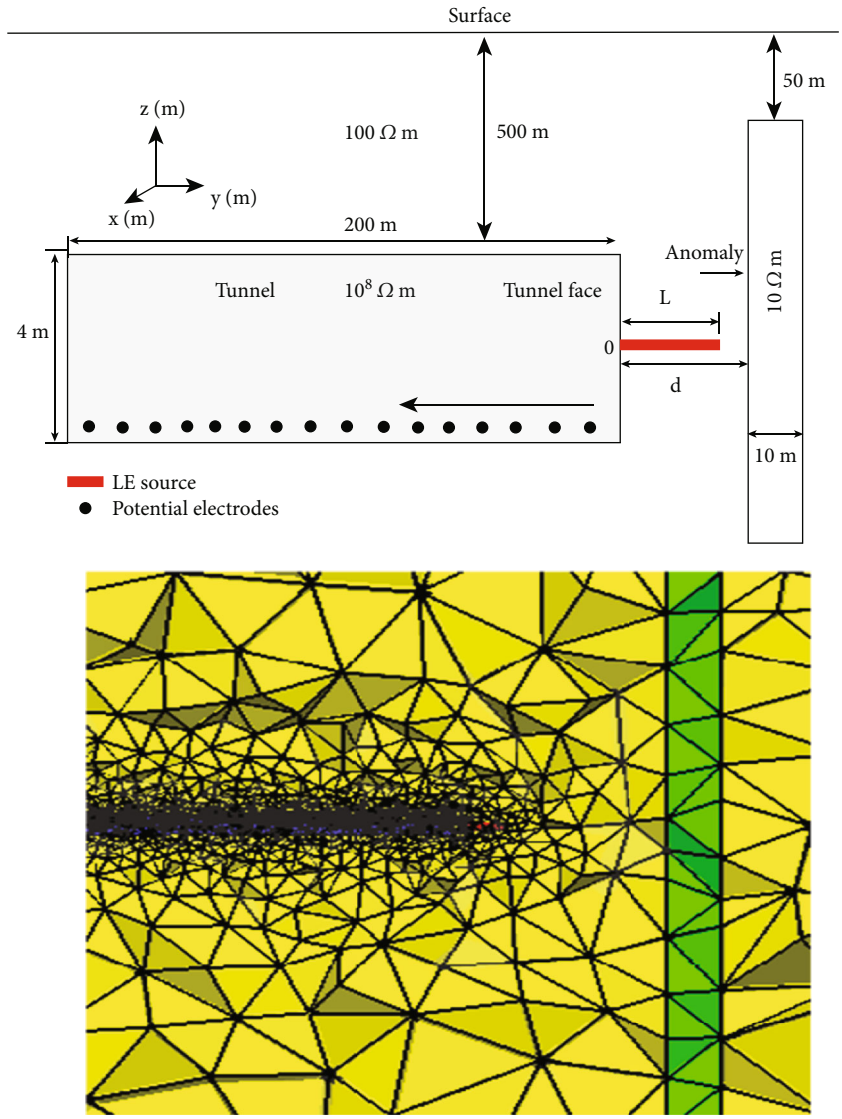

Figure 6: Numerical model of LE source and its finite element mesh.

prediction model for the LE source is based on the pole-dipole array.

Figure 5 shows the results of this prediction model by Equation (6). The colored dots represent the numerical results of the predicted distance from the minimum offset, and the lines represent the real distance of the fault anomaly. Most of the predicted results are consistent with the real fault distance, and the error of a few points is small, which indicates that the fitting of the prediction equation is accurate.

Table 1 lists detailed data information, which shows the specific impact of the actual distance and the length of the LE source on the apparent resistivity curve and error analysis from the prediction model. The maximum error of only one point is 6.33%, and the result error of 91.6% is acceptable. The proposed prediction equation introduces firstly the LE source into detecting the fault anomaly in the tunnel. The LE source way can be used quantitatively to estimate the location of the anomaly, which increases the detection ability

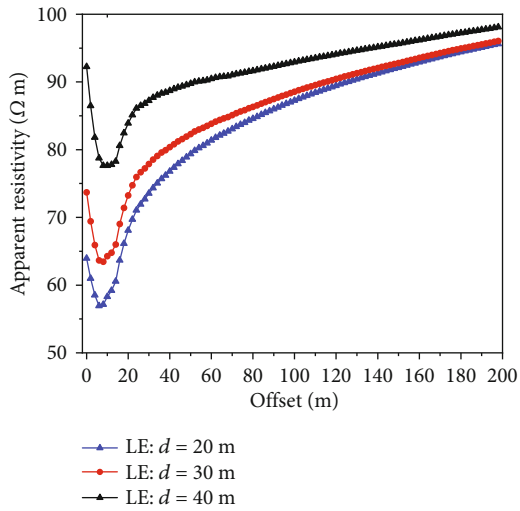

Figure 7: Apparent resistivity profiles of the LE source.

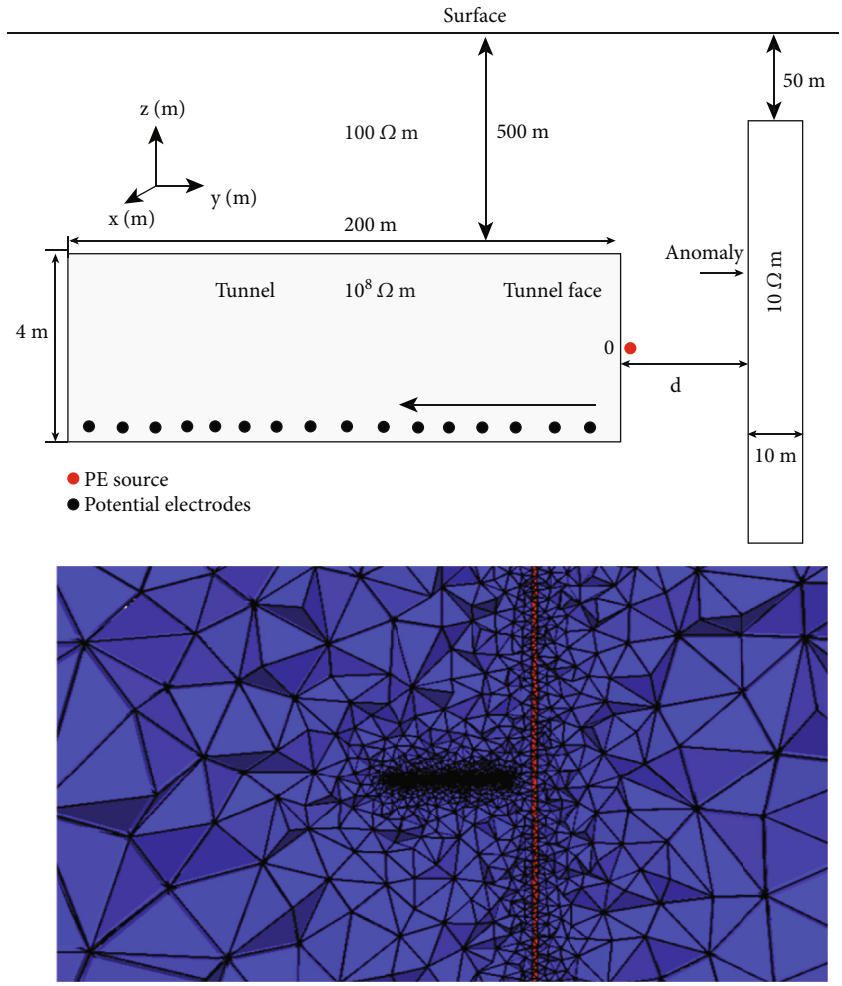

Figure 8: Numerical model of PE source and its finite element mesh.

to the water-rich fault and improves the construction efficiency. The LE source can still observe obvious anomaly signal of apparent resistivity curve when the real horizontal distance reaches 120 m, which indicates that the LE prediction model has good applicability ability for detecting the long-distance anomaly.

4.2. Comparison of Prediction Models. Next, we discuss the comparison of the prediction models calculated by the LE source method and the PE source method. For more convenience in comparisons of prediction models between the LE source and PE source, the prediction formula of the PE source method is given [3].

$$d^{\text{pre}} = f(x_{\min}, \lambda) = c_1 x_{\min} + c_2 + c_3 \lambda, \tag{7}$$

where d^{pre} represents the predicted distance of anomaly, $x_{\min}$ is the offset of the minimum apparent resistivity, λ represents the anisotropic coefficient ($\lambda = 1$), and the coefficients are $c_1 = 0.302$, $c_2 = 0.802$, and $c_3 = -1.48$.

First of all, the LE source model is simulated. It is assumed that there is a vertical fault anomaly in front of the tunnel face, which is used to simulate the low resistance distribution of the water-bearing fault, and then the PE source model is simulated to compare the LE source model. The LE source is located at point O. Its model has been shown in Figure 6, The thickness of the fault is 10 m, and the depth of tunnel is 500 m, the tunnel size is 200 m × 4 m × 4 m, the air of tunnel has a resistivity of $10^8\,\Omega$ m, and a lot of potential electrodes are placed at the tunnel floor with an interval of 2 m. The surrounding rock is 100 Ω m, and the fault is 10 Ω m. The fault dimension is 1800 m × 10 m × 900 m, and the whole model domain is enough large. By changing the horizontal distance of the fault ($d = 20$ m, 30 m, 40 m) and keeping the LE source with a length of $L = 5$ m, we calculated three LE source models. Behind the tunnel face, 100 potential electrodes are used to observe the results.

Figure 7 shows the apparent resistivity results of the LE source method with the actual horizontal distance of 20 m, 30 m, and 40 m, respectively. We can know that when the real horizontal distance is small ($d = 20$ m), the offset corresponding to the abscissa of the minimum apparent resistivity is also small. Besides, with the increase of the actual distance, the offset corresponding to the abscissa of the minimum apparent resistivity also rises, and the relative

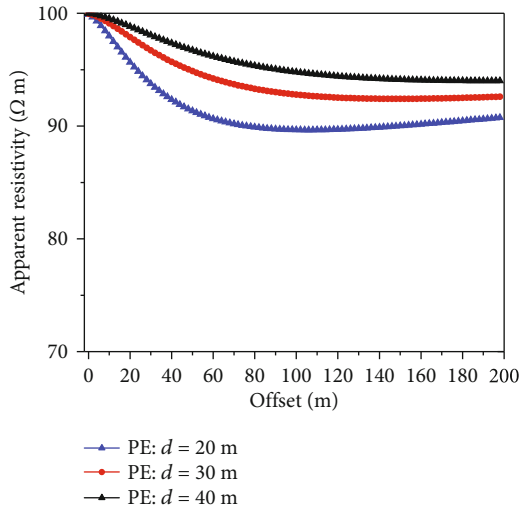

Figure 9: Apparent resistivity profiles of the PE source at different distances.

amplitude of the anomaly response becomes smaller and smaller. But the low resistivity signal of apparent resistivity at $d = 20$ m can still be observed. This is consistent with the trend of the PE source [6, 32].

To compare the detection effect of the LE source method and the PE source method under the same conditions, a PE source is arranged at the same position of the tunnel face as the above LE model. Liu and Wu [32] mentioned that the PE source method has a small detection depth for the anomaly due to the inaccessibility of the tunnel face. Therefore, the fault water-bearing anomaly is assumed at different distances ahead of the face as a comparative discussion, and the PE model is shown in Figure 8.

Figure 9 shows the apparent resistivity curves of the PE source method with the actual horizontal distance of 20 m, 30 m, and 40 m, respectively. We can see that when the actual horizontal distance is distributed in a short distance ($d = 20$ m), the curve can also observe the offset position of the minimum value, which indicates that the PE source can detect the anomaly at this depth. However, when the actual horizontal distance is 40 m, it is hard to find the minimum offset in the apparent resistivity curve, which means that the detection effect of the PE source at a large depth is not ideal.

Figure 10 shows the numerically predicted results obtained by the above LE prediction model and PE prediction model [3]. The colored lines represent the actual horizontal distance of the fault, the red triangle points denote the predicted distances of the LE prediction model, and the blue dots denote the predicted distance obtained from the PE prediction model.

Table 2 shows the detailed results and error analysis of the predicted distances calculated by the prediction models of the LE source and PE source. The results show that the predicted distance error of the LE source is small, and the absolute value of the maximum error is not more than 3.72%. It can accurately predict the position of both a short-distance anomaly and a long-distance anomaly. The distance error calculated by the PE source is very accurate

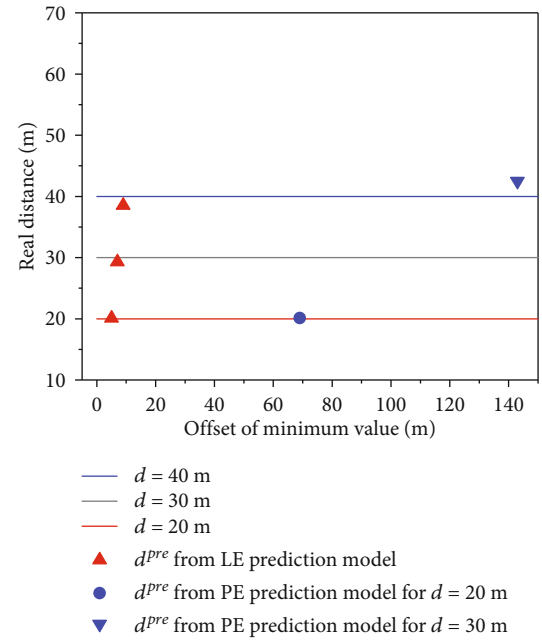

Figure 10: Fitted results of the LE prediction model and PE prediction model for tunnel detection.

Table 2: Predicted results of LE and PE prediction models for tunnel detection and their errors.

Distance (m)	Prediction model	Offset (m)	Predicted distance (m)	Error (%)
$d = 20$	PE	$x_{min} = 69$	$d^{pre} = 20.16$	0.80
$d = 20$	LE ($L = 5$ m)	$x_{min} = 5$	$d^{pre} = 20.09$	0.45
$d = 30$	PE	$x_{min} = 143$	$d^{pre} = 42.50$	41.6
$d = 30$	LE ($L = 5$ m)	$x_{min} = 7$	$d^{pre} = 29.30$	-2.33
$d = 40$	PE	/	/	/
$d = 40$	LE ($L = 5$ m)	$x_{min} = 9$	$d^{pre} = 38.51$	-3.72

at a short distance ($d = 20$ m) with only 0.80% error. But the predicted distance does not match the real distance of the fault at a long distance ($d = 30$ m). Therefore, the effective detection depth of the LE source prediction model is greater than that of the PE source. This method is the innovation and development of the PE source prediction model for tunnel exploration under the favorable conditions of using pilot drilling.

5. Conclusion

In the process of tunnel excavation, owing to the impermeability of the tunnel face, the detection effect of the conventional PE source for a long-distance anomaly ahead of the tunnel face is limited, and it could not accurately detect the location of the remote anomaly in front of the tunnel. Based on three-dimensional modeling of the LE source resistivity method, this paper simulates a fault model ahead of the tunnel, obtains apparent resistivity curves response of the LE source method, and uses the

minimum offset to put forward the prediction model of the LE source in the tunnel. The errors of 91.6% predicted distances calculated by the LE source are very small, which indicates that the LE source prediction model is accurate and reliable. It can quantitatively guide the tunnel surveyors with the LE source method to estimate the position of the remote water-containing disaster anomaly. The simulated results show that the offset value corresponding to abscissa of the minimum apparent resistivity can still be extracted for the anomaly with a distance of 120 m, which demonstrates that the LE source method has good adaptability and detection ability for the long-distance anomaly. Based on the same parameters, comparisons of the LE source and PE source show that the prediction model of the LE source can accurately estimate the remote anomaly location. The LE source method makes good use of the tunnel horizontal pilot drilling hole to increase the detection signal and detection depth. It can improve the construction efficiency, and effectively prevent water inrush in the tunnel. In the practical application of tunnel exploration, it is recommended to widely use the LE source method.

Data Availability

The data that support the findings of this study are available from the corresponding author upon reasonable request.

Conflicts of Interest

The authors declare no conflicts of interest.

Acknowledgments

This work was supported in part by the Major Science and Technology Projects of the Ministry of Water Resources (SKS-2022028) and the National Key R&D Program of China (no. 2018YFE0208300).

References

[1] B. Liu, S. Li, S. Li, and S. Zhong, "Study of advance detection of water-bearing geological structureswith DC resistivity method," *Rock and Soil Mechanics*, vol. 30, no. 10, pp. 3093–3101, 2009.

[2] J. H. Yue, H. Yang, and B. Y. Su, "Theoretical foundation of tensor measurement for mine resistivity method," *Journal of China Coal Social*, vol. 45, no. 7, pp. 2464–2471, 2020.

[3] D. M. Hu, X. D. Yang, M. Yue, Y. Li, and X. P. Wu, "Prediction model for advanced detection of water-rich faults using 3D anisotropic resistivity modeling and Monte Carlo methods," *IEEE Access*, vol. 9, no. 2, pp. 18251–18261, 2021.

[4] G. Xue, Y. Yan, X. Li, and Q. Di, "Transient electromagnetic S-inversion in tunnel prediction," *Geophysical Research Letters*, vol. 34, no. 18, pp. 529–538, 2007.

[5] S. Li, B. Liu, L. Nie et al., "Detecting and monitoring of water inrush in tunnels and coal mines using direct current resistivity method: a review," *Journal of Rock Mechanics and Geotechnical Engineering*, vol. 7, no. 4, pp. 469–478, 2015.

[6] J. Huang, J. Wang, and B. Ruan, "Anomalous of large polar distance dipole-dipole resistivity sounding in tunnel," *Progress in Geophysics*, vol. 6, no. 22, pp. 1935–1941, 2007.

[7] B. Y. Ruan, X. K. Deng, H. F. Liu, L. Zhou, and L. Zhang, "Research on a new method of advanced focus detection with dc resistivity in tunnels," *Chinese Journal of Geophysics*, vol. 52, no. 1, pp. 250–259, 2009.

[8] W. Daily, A. Ramirez, R. Newmark, and K. Masica, "Low-cost reservoir tomographs of electrical resistivity," *The Leading Edge*, vol. 23, no. 5, pp. 472–480, 2004.

[9] D. Rucker, M. Loke, M. Levitt, and G. Noonan, "Electrical-resistivity characterization of an industrial site using long electrodes," *Geophysics*, vol. 75, no. 4, p. WA95, 2010.

[10] C. Weiss, D. Aldridge, H. Knox, K. Schramm, and L. Bartel, "The direct-current response of electrically conducting fractures excited by a grounded current source," *Geophysics*, vol. 81, no. 3, pp. E201–E210, 2016.

[11] M. H. Loke, J. E. Chambers, D. F. Rucker, O. Kuras, and P. Wilkinson, "Recent developments in the direct-current geoelectrical imaging method," *Journal of Applied Geophysics*, vol. 95, no. 4, pp. 135–156, 2013.

[12] S. Ullah, B. Zhou, and M. A. Iqbal, "A novel electrode array for electrical resistivity tomography to assess groundwater resources: field test at Liwa UAE," *Journal of Environmental Engineering and Science*, vol. 15, pp. 1–11, 2020.

[13] J. H. Coggon, "Electromagnetic and electrical modeling by the finite element method," *Geophysics*, vol. 36, no. 1, pp. 132–155, 1971.

[14] H. M. Bibby, "Direct current resistivity modeling for axially symmetric bodies using the finite-element method," *Geophysics*, vol. 43, no. 3, pp. 550–562, 1978.

[15] Y. Wang, M. Yan, and W. Song, "The effect of cyclic stress amplitude on macro-meso failure of rock under triaxial confining pressure unloading," *Fatigue & Fracture of Engineering Materials & Structures*, vol. 47, no. 12, pp. 3008–3025, 2023.

[16] P. Queralt, J. Pous, and A. Marcuello, "2-D resistivity modeling, an approach to arrays parallel to the strike direction," *Geophysics*, vol. 56, no. 7, pp. 941–950, 1991.

[17] Y. Wang, P. F. Tan, J. Han, and P. Li, "Energy-driven fracture and instability of deeply buried rock under triaxial alternative fatigue loads and multistage unloading conditions: prior fatigue damage effect," *International Journal of Fatigue*, vol. 168, no. 407410, p. 107410, 2023.

[18] Y. Wang, Z. Cao, P. Li, and X. Yi, "On the fracture and energy characteristics of granite containing circular cavity under variable frequency-amplitude fatigue loads," *Theoretical and Applied Fracture Mechanics*, vol. 125, article 103872, 2023.

[19] Y. Li and K. Spitzer, "Three-dimensional DC resistivity forward modelling using finite elements in comparison with finite-difference solutions," *Geophysical Journal International*, vol. 151, no. 3, pp. 924–934, 2002.

[20] C. Yin and P. Weidelt, "Geoelectrical fields in a layered earth with arbitrary anisotropy," *Geophysics*, vol. 64, no. 2, pp. 426–434, 1999.

[21] C. C. Pain, J. V. Herwanger, J. H. Saunders, M. H. Worthington, and C. R. de Oliveira, "Anisotropic resistivity inversion," *Inverse Problems*, vol. 19, no. 5, pp. 1081–1111, 2003.

[22] Y. Li and K. Spitzer, "Finite element resistivity modelling for three-dimensional structures with arbitrary anisotropy," *Physics of the Earth and Planetary Interiors*, vol. 150, no. 1-3, pp. 15–27, 2005.

[23] Z. Ren, L. Qiu, J. Tang, X. Wu, and X. Zhou, "3D direct current resistivity anisotropic modelling by goal-oriented adaptive finite element methods," *Geophysical Journal International*, vol. 212, no. 1, pp. 76–87, 2018.

[24] Y. Sasaki, "3D resistivity inversion using the finite-element method," *Geophysics*, vol. 59, no. 12, pp. 1839–1848, 1994.

[25] M. Yi, J. Kim, Y. Song, S. Cho, S. Chung, and J. Suh, "Three-dimensional imaging of subsurface structures using resistivity data," *Geophysical Prospecting*, vol. 49, no. 4, pp. 483–497, 2001.

[26] J. R. Shewchuk, "Delaunay refinement algorithms for triangular mesh generation," *Comput. Geometry—Theory and Applications*, vol. 22, no. 1-3, pp. 21–74, 2002.

[27] C. Rücker, T. Günther, and K. Spitzer, "Three-dimensional modelling and inversion of dc resistivity data incorporating topography - I. Modelling," *Geophysical Journal International*, vol. 166, no. 2, pp. 495–505, 2006.

[28] K. Key and C. Weiss, "Adaptive finite-element modeling using unstructured grids: the 2D magnetotelluric example," *Geophysics*, vol. 71, no. 6, pp. G291–G299, 2006.

[29] E. Erdoğan, I. Demirci, and M. E. Candansayar, "Incorporating topography into 2d resistivity modeling using finite-element and finite-difference approaches," *Geophysics*, vol. 73, no. 3, pp. F135–F142, 2008.

[30] Z. Ren and J. Tang, "A goal-oriented adaptive finite-element approach for multi-electrode resistivity system," *Geophysical Journal International*, vol. 199, no. 1, pp. 136–145, 2014.

[31] J. A. Stratton, *Electromagnetic Theory*, John Wiley and Sons, New Jersey, 2007.

[32] Y. Liu and X. Wu, "Parallel Monte Carlo method for advanced detection in tunnel incorporating anisotropic resistivity effect," *Chinese Journal of Geophysics*, vol. 59, no. 11, pp. 4297–4309, 2016.

[33] J. Yang, Y. Liu, and X. Wu, "3-D DC resistivity modelling with arbitrary long electrode sources using finite element method on unstructured grids," *Geophysical Journal International*, vol. 211, no. 2, pp. 1162–1176, 2017.

[34] W. Wang, X. Wu, and K. Spitzer, "Three-dimensional DC anisotropic resistivity modelling using finite elements on unstructured grids," *Geophysical Journal International*, vol. 193, no. 2, pp. 734–746, 2013.

[35] Q. L. Shi, *Calculus*, Chongqing University Press, Chongqing, 2017.

[36] D. Hu, T. Bülent, and M. Yue, "A new method of 3D direct current resistivity modelling using a long electrode source for forward probing in tunnels," *Near Surface Geophysics*, vol. 20, no. 6, pp. 590–606, 2022.

[37] A. Franke, R. Börner, and K. Spitzer, "Adaptive unstructured grid finite element simulation of two-dimensional magnetotelluric fields for arbitrary surface and seafloor topography," *Geophysical Journal of the Royal Astronomical Society*, vol. 171, no. 1, pp. 71–86, 2007.

[38] Z. Ren and J. Tang, "3D direct current resistivity modeling with unstructured mesh by adaptive finite-element method," *Geophysics*, vol. 75, no. 1, pp. H7–H17, 2010.